CrossMark

Electro-Magnetohydrodynamic Oscillatory Flow of a Dielectric Fluid Through a Porous Medium with Heat Transfer: Brinkman Model

R. E. Abo-Elkhair[1] · Kh. S. Mekheimer[1] · A. Z. Zaher[2]

Abstract

The objective of the present study is to investigate the effect of electro-magnetic field and heat transfer on the oscillatory flow of a dielectric fluid through a Darcy's Brinkman model in a symmetric flexible sinusoidal wavy channel. The equations which govern the Electro-Magneto hydro dynamic of oscillatory flow for a dielectric fluid are made non-dimensional and coordinate transformation is employed to convert the irregular boundary to a regular boundary. The obtained system of equations is solved analytically by using the regular perturbation method with a small amplitude ratio. Approximate solution for the mean axial velocity, the mean electric potential, the mean temperature, and the mean pressure gradient is obtained. Further, the effect of pertinent parameters is demonstrated and discussed. The phenomena of reflux (the mean flow reversal) are discussed. It is found that the critical reflux pressure is greater for a fluid without an electric field. Also, the increase of magnetic field decreases the flow rate which is helpful to control the blood flow during the surgeries.

Keywords Peristaltic transport · Dielectric fluid · Heat transfer · Electro-magnetic field · Porous medium · Brinkman model

1 Introduction

Electro kinetics "electro-fluid dynamics (EFD) or electro hydrodynamics (EHD)" is the study of the dynamics of electrically charged fluids. In addition, it is the study of the motions of ionized particles or molecules and their interactions with electric fields and the surrounding fluid. Electro hydrodynamics EHD covers the following types of particle and fluid transport mechanisms: electrophoresis, electro kinesis, dielectrophoresis, electro-osmosis, and electrorotation. It appears in many applications such as enhancement of drying rates, drag reduction, plasma actuators, and gas pumps. Electro hydrodynamics EHD equations of motion can be classified to two groups: hydrodynamic equations and electric field equations. Theoretically, electro hydrodynamics EHD flow was investigated by Woodson and Melcher [1]. The problem of the onset of convective instability in a horizontal layer of a dielectric fluid under a simultaneous action of a vertical alternative current AC electric field and a vertical temperature gradient was examined by Takashima [2, 3] and Vidhya et. al [4]. Also, the effect of vertical alternative current AC electric field and heat transfer on peristaltic flow of a viscous incompressible dielectric liquid sheet in asymmetrical flexible channel has been investigated by el-sayed et al. [5].

The temperature is associated with the motion of molecules within a fluid [6], being directly related to the kinetic energy of the molecules, including vibrational and rotational motion. Heat transfer is the energy transferred between two points at different temperatures. It has significant in several industrial and medical applications such as heat conduction in tissues, heat transfer due to

✉ R. E. Abo-Elkhair
elkhair33@yahoo.com

Kh. S. Mekheimer
kh_Mekheimer@yahoo.com; kh_Mekheimer@azhar.edu.eg

A. Z. Zaher
abdullah.zaher@feng.bu.edu.eg

[1] Mathematics Department, Faculty of Science, Al-Azhar University, Nasr City, 11884, Cairo, Egypt

[2] Engineering Mathematics and Physics Department, Faculty of Engineering - Shubra- Benha University, Cairo, Egypt

perfusion of the arterial-venous blood through the pores of the tissue, metabolic heat generation, and external interactions such as electromagnetic radiation emitted from cell phones. Also, thermodynamic aspects of blood may become significant in processes like oxygenation and hemodialysis when blood is drawn out of the body. Considering the needs of investigations in the peristaltic movement of physiological fluids, many authors [7–16] have been studied peristaltic flow with heat transfer.

Peristaltic flow of magnetohydrodynamic (MHD) fluid plays very important role in medical sciences and bio engineering such as cancer tumor treatment, cell separation, and blood reduction during surgeries. The effect of moving magnetic field on peristaltic flow is studied by many authors [17–24]. The magneto hydrodynamic (MHD) and electro hydrodynamics (EHD) flows through porous tube are great interest in the study of the interaction of the geomagnetic and electric fields with the blood in the oscillatory flow. Flow through a porous medium has several practical applications especially in geophysical fluid dynamics. Moreover, the natural porous media are modeled as beach sand, sandstone, limestone, the human lung, bile duct, and gall bladder with stones in small blood vessels. El Shehawey et. al. [25, 26] studied the peristaltic flow of a Newtonian fluid thorough a porous medium. There are distinct types for porous media such as Darcy's, Forchheimer's and Brinkman's models. In the proposed system, we focus on the Brinkman model because of its many objectives. One of the objectives is to examine flow structure near the bounding walls. Our second objective is to test the feasibility of addressing the thin region. The Darcy-Brinkman model is interest in biomedical hydrodynamic studies, including its use in modeling a thin fibrous surface layer coating blood vessels (endothelial surface layer) as it is a highly permeable, high porosity porous medium [27].

Increasing the exploitation of technologies that use electric magnetic fields in some specific branches such as medicine based on magnetic resonance imaging and transportation systems that use direct current, in addition it is used in cancer treatment, so we found that it is important to study the electro-magnetohydrodynamic oscillatory flow of a dielectric fluid through a porous medium (Brinkman's model) in the presence of the heat transfer. Accordingly, in the present work, we study the effect of the interaction between the Electro Hydrodynamics (EHD) and magnetohydrodynamic (MHD) in peristaltic flow through porous medium with heat transfer by considering a small wave number . The velocity profile, temperature distribution, pressure gradient, the critical pressure, and electric potential function are obtained, by using the regular perturbation method up to the second order in terms of the amplitude ratio and wave number.

2 Equations of Motion

We consider a symmetric two-dimensional channel of uniform width $2d$ filled with an incompressible dielectric fluid. We assume an infinite sinusoidal wave train traveling along the walls. The lower and the upper walls are maintained at constant temperatures θ_{00} and θ_{10}, respectively. In addition to the temperature gradient, a vertical a.c. electric field is also imposed across the channel. The lower wall is grounded and the upper wall is kept at the electric potential φ_{10}. Also

Fig. 1 Sketch of the physical model
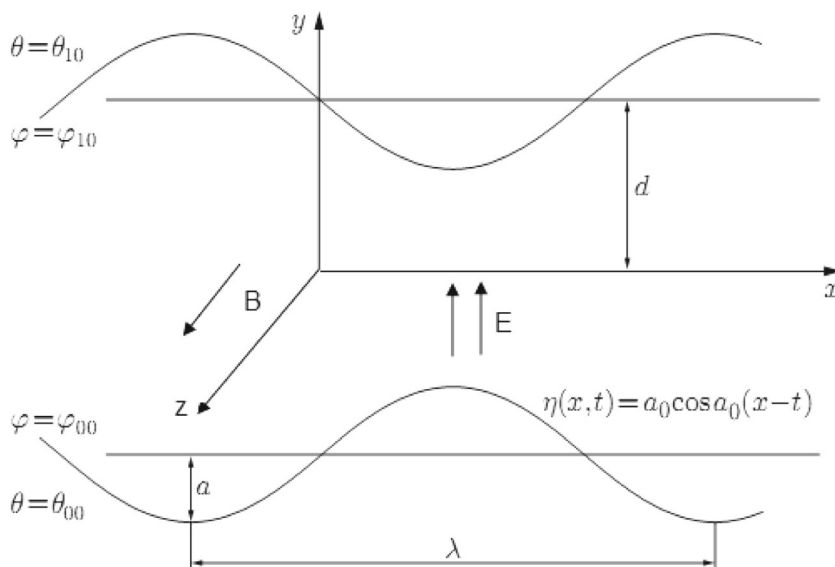
we apply a constant magnetic field perpendicular to the electric field as shown in Fig. 1

$$h'(X', t') = d + a \cos \frac{2\pi}{\lambda}\left(x - \frac{\kappa}{d}t\right), \tag{1}$$

where d, a, λ, $\frac{\kappa}{d}$ and t are width, amplitude, wavelength, velocity of the wave and time. In the absence of external forces and the fluid in the porous structure then equations of continuity and momentum for the flow of an incompressible fluid are given by Brinkman's equations in the following form,

$$\nabla . \vec{q} = 0, \tag{2}$$

$$\rho\left(\frac{\partial \vec{q}}{\partial t} + (\vec{q}.\nabla)\vec{q}\right) = -\nabla p^* + \mu_1 \nabla^2 \vec{q} - \frac{\mu}{k_1}\vec{q} + \vec{J} \times \vec{B} + \vec{f}_e, \tag{3}$$

$$\frac{\partial \theta}{\partial t} + \vec{q}.\nabla \theta = \kappa \nabla^2 \theta, \tag{4}$$

$$\vec{f}_e = \rho_e \vec{E} - \frac{1}{2}E^2 \nabla \varepsilon + \frac{1}{2}\nabla\left(\rho\frac{\partial \varepsilon}{\partial \rho}E^2\right), \tag{5}$$

$$\vec{J} = \sigma^*\left[\vec{q} \times \vec{B} - \frac{1}{e_1 n_e}\vec{J} \times \vec{B}\right], \tag{6}$$

where $\mu_1 = \frac{\mu}{e}$, $\vec{q}$, ρ, p^*, ν, θ, $\kappa = \frac{K}{\rho c}$, K, c, $\vec{f}_e$, ρ_e, $\vec{E}$, ε, $\vec{J}$, $\vec{B}$, σ^*, e_1, e, k_1 and n_e are apparent viscosity of the fluid, velocity vector of the fluid, density, pressure, kinematic viscosity, temperature, thermometric conductivity, thermal conductivity, specific heat, body forces of electrical origin per unit volume, free charge density, electric field, dielectric constant, current density, total magnetic field, electric conductivity, electric charge, the porosity parameter, permeability coefficient, and the number of electrons density.

Since there is no free charge, The Maxwell's equation following [28] are:

$$\nabla \cdot (\varepsilon \vec{E}) = 0,$$
$$\nabla \times \vec{E} = 0, \ \text{ or } \ \vec{E} = -\nabla \varphi, \tag{7}$$

where φ is the electric potential, and the dielectric constant ε is assumed to be a function of temperature as follows [3],

$$\varepsilon = \varepsilon_0(1 - \epsilon(\theta - \theta_{00})).$$

Then, the governing equations for two-dimensional motion of this model are:

$$\frac{\partial u}{\partial t} + u\frac{\partial u}{\partial x} + v\frac{\partial u}{\partial y} = -\frac{1}{\rho}\frac{\partial p}{\partial x} + \frac{\nu}{e}\nabla^2 u - \frac{\nu}{k_1}u$$
$$+ \frac{\sigma^* B_0^2}{1 + m^2}(mv - u) + \frac{\varepsilon_0 \epsilon}{2\rho}\left(\frac{\partial \varphi}{\partial y}\right)^2\frac{\partial \theta}{\partial x},$$

$$\frac{\partial v}{\partial t} + u\frac{\partial v}{\partial x} + v\frac{\partial v}{\partial y} = -\frac{1}{\rho}\frac{\partial p}{\partial y} + \frac{\nu}{e}\nabla^2 v - \frac{\nu}{k_1}v$$
$$- \frac{\sigma^* B_0^2}{1 + m^2}(mu + v) + \frac{\varepsilon_0 \epsilon}{2\rho}\left(\frac{\partial \varphi}{\partial y}\right)^2\frac{\partial \theta}{\partial y},$$

$$\frac{\partial \theta}{\partial t} + u\frac{\partial \theta}{\partial x} + v\frac{\partial \theta}{\partial y} = \kappa \nabla^2 \theta, \frac{\partial}{\partial y}\left[(1 - \epsilon(\theta - \theta_{00}))\frac{\partial \varphi}{\partial y}\right] = 0, \tag{8}$$

where ε_0 be the permittivity at vacuum , ϵ be the thermal expansion coefficients of dielectric constant ε and $p = p^* - \frac{1}{2}(\rho E^2 \frac{\partial \varepsilon}{\partial \rho})$. We introduce the stream function $u = \frac{\partial \psi}{\partial y}$, $v = -\frac{\partial \psi}{\partial x}$, then we find

$$\frac{\partial^2 \psi}{\partial t \partial y} + \frac{\partial \psi}{\partial y}\frac{\partial^2 \psi}{\partial x \partial y} - \frac{\partial \psi}{\partial x}\frac{\partial^2 \psi}{\partial y^2} = -\frac{1}{\rho}\frac{\partial p}{\partial x} + \frac{\nu}{e}\nabla^2\frac{\partial \psi}{\partial y}$$
$$- \frac{\nu}{k_1}\frac{\partial \psi}{\partial y} + \frac{\sigma^* B_0^2}{1 + m^2}\left(-m\frac{\partial \psi}{\partial x} - \frac{\partial \psi}{\partial y}\right) + \frac{\varepsilon_0 \epsilon}{2\rho}\left(\frac{\partial \varphi}{\partial y}\right)^2\frac{\partial \theta}{\partial x},$$

$$\frac{\partial \psi}{\partial x}\frac{\partial^2 \psi}{\partial y \partial x} - \frac{\partial^2 \psi}{\partial t \partial x} - \frac{\partial \psi}{\partial y}\frac{\partial^2 \psi}{\partial x^2} = -\frac{1}{\rho}\frac{\partial p}{\partial y} - \frac{\nu}{e}\nabla^2\frac{\partial \psi}{\partial x} + \frac{\nu}{k_1}\frac{\partial \psi}{\partial x}$$
$$- \frac{\sigma^* B_0^2}{1 + m^2}\left(m\frac{\partial \psi}{\partial y} - \frac{\partial \psi}{\partial x}\right) + \frac{\varepsilon_0 \epsilon}{2\rho}\left(\frac{\partial \varphi}{\partial y}\right)^2\frac{\partial \theta}{\partial y}, \tag{9}$$

$$\frac{\partial \theta}{\partial t} + \frac{\partial \psi}{\partial y}\frac{\partial \theta}{\partial x} - \frac{\partial \psi}{\partial x}\frac{\partial \theta}{\partial y} = \kappa \nabla^2 \theta,$$
$$\frac{\partial}{\partial y}\left[(1 - \epsilon(\theta - \theta_{00}))\frac{\partial \varphi}{\partial y}\right] = 0.$$

For further analysis, we use the following non-dimensional variables and parameters:

$$x = \frac{x'}{d}, y = \frac{y'}{d}, u = \frac{u'd}{\kappa}, v = \frac{v'd}{\kappa}, \eta = \frac{\eta'}{d}, p = \frac{d^2 p'}{\rho \kappa^2},$$
$$t = \frac{\kappa t'}{d^2}, \psi = \frac{\psi'}{\kappa}, \theta = \frac{\theta'}{\beta d}, \varphi = \frac{\varphi'}{E_0 d}, \gamma = \frac{L}{L_2 R}. \tag{10}$$

Using the non-dimensional variables and parameters given above in Eq. 9, we find that the equations which govern the flow for a fluid in terms of the stream function $\psi(x, t)$

$$\frac{\partial^2 \psi}{\partial t \partial y} + \frac{\partial \psi}{\partial y}\frac{\partial^2 \psi}{\partial x \partial y} - \frac{\partial \psi}{\partial x}\frac{\partial^2 \psi}{\partial y^2} = -\frac{\partial p}{\partial x} + \frac{1}{eR_e}\nabla^2\frac{\partial \psi}{\partial y} - \frac{1}{R_e \sigma}\frac{\partial \psi}{\partial y}$$
$$+ \frac{M}{R_e(1 + m^2)}\left(-m\frac{\partial \psi}{\partial x} - \frac{\partial \psi}{\partial y}\right) + \frac{\gamma}{2}\left(\frac{\partial \varphi}{\partial y}\right)^2\frac{\partial \theta}{\partial x},$$

$$\frac{\partial \psi}{\partial x}\frac{\partial^2 \psi}{\partial y \partial x} - \frac{\partial^2 \psi}{\partial t \partial x} - \frac{\partial \psi}{\partial y}\frac{\partial^2 \psi}{\partial x^2} = -\frac{\partial p}{\partial y} - \frac{1}{eR_e}\nabla^2\frac{\partial \psi}{\partial x}$$
$$+ \frac{1}{R_e \sigma}\frac{\partial \psi}{\partial x} - \frac{M}{R_e(1 + m^2)}\left(m\frac{\partial \psi}{\partial y} - \frac{\partial \psi}{\partial x}\right) + \frac{\gamma}{2}\left(\frac{\partial \varphi}{\partial y}\right)^2\frac{\partial \theta}{\partial y},$$

$$\frac{\partial \theta}{\partial t} + \frac{\partial \psi}{\partial y}\frac{\partial \theta}{\partial x} - \frac{\partial \psi}{\partial x}\frac{\partial \theta}{\partial y} = \nabla^2 \theta,$$
$$\frac{\partial}{\partial y}\left[(1 - \epsilon(\theta - \theta_{00}))\frac{\partial \varphi}{\partial y}\right] = 0. \tag{11}$$

Where $R = \frac{\kappa}{\nu} = \frac{cd}{\nu}$ is the Reynolds number , $L = \frac{\varepsilon_0 E_0^2 d^2(\epsilon \beta d)^2}{\mu \kappa}$ is electrical Rayleigh number, $L_2 = \epsilon \beta d$, $\beta = \frac{\theta_{00} - \theta_{10}}{2d}$ is adverse temperature gradient, $M = \frac{\sigma^* B_0^2 d^2}{\nu}$ is the Hartmann number , $m = \frac{\sigma^* B_0}{e_1 n_e}$ is the Hall parameter, $\sigma = \frac{k_1}{d^2}$ is the permeability parameter, $a_0 = \frac{a}{d}$ is amplitude ratio and $\alpha_0 = \frac{2\pi d}{\lambda}$ is the wave number.

The corresponding dimensionless boundary conditions are

$$\frac{\partial \psi}{\partial y} = 0 \;,\quad \frac{\partial \psi}{\partial y} = -a_0\alpha_0 \sin\alpha_0(x-t),\quad \theta = \frac{\theta_{10}}{\beta d}\;,\quad \varphi = \frac{\varphi_{10}}{E_0 d}\quad at\;\; y = 1+\eta,$$

$$\frac{\partial \psi}{\partial y} = 0 \;,\quad \frac{\partial \psi}{\partial y} = a_0\alpha_0 \sin\alpha_0(x-t)\;,\quad \theta = \frac{\theta_{00}}{\beta d}\;,\quad \varphi = \frac{\varphi_{00}}{E_0 d}\quad at\;\; y = -(1+\eta),$$

(12)

where $\eta = a_0 \sin\alpha_0(x-t)$.

3 Solution of the Problem

We assume that the dimensionless quantities ψ, p, θ and φ can be expanded, respectively, in powers of the amplitude ratio a_0 as follows [29]:

$$\psi = \psi_0 + a_0\psi_1 + a_0^2\psi_2,$$
$$\theta = \theta_0 + a_0\theta_1 + a_0^2\theta_2,$$
$$p = p_0 + a_0 p_1 + a_0^2 p_2,$$
$$\varphi = \varphi_0 + a_0\varphi_1 + a_0^2\varphi_2,$$
$$\frac{\partial p}{\partial x} = \frac{\partial p_0}{\partial x} + a_0\frac{\partial p_1}{\partial x} + a_0^2\frac{\partial p_2}{\partial x},$$

(13)

where $\frac{\partial p}{\partial x}$ be the pressure gradient. Substituting Eq. 13 into Eqs. 11 and 12 and collecting terms of equal powers of a_0, we obtain the following set of the system model.

Zeroth-Order System Model

$$\frac{\partial^2\psi_0}{\partial t\partial y} + \frac{\partial\psi_0}{\partial y}\frac{\partial^2\psi_0}{\partial x\partial y} - \frac{\partial\psi_0}{\partial x}\frac{\partial^2\psi_0}{\partial y^2} = -\frac{\partial p_0}{\partial x} + \frac{1}{eR_e}\nabla^2\frac{\partial\psi_0}{\partial y}$$
$$-\frac{1}{R_e\sigma}\frac{\partial\psi_0}{\partial y} + \frac{M}{R_e(1+m^2)}\left(-m\frac{\partial\psi_0}{\partial x} - \frac{\partial\psi_0}{\partial y}\right) + \frac{\gamma}{2}\left(\frac{\partial\varphi_0}{\partial y}\right)^2\frac{\partial\theta_0}{\partial x},$$

$$\frac{\partial\psi_0}{\partial x}\frac{\partial^2\psi_0}{\partial x\partial y} - \frac{\partial^2\psi_0}{\partial t\partial x} - \frac{\partial\psi_0}{\partial y}\frac{\partial^2\psi_0}{\partial x^2} = -\frac{\partial p_0}{\partial y} - \frac{1}{eR_e}\nabla^2\frac{\partial\psi_0}{\partial x}$$
$$+\frac{1}{R_e\sigma}\frac{\partial\psi_0}{\partial x} - \frac{M}{R_e(1+m^2)}\left(-m\frac{\partial\psi_0}{\partial y} - \frac{\partial\psi_0}{\partial x}\right) + \frac{\gamma}{2}\left(\frac{\partial\varphi_0}{\partial y}\right)^2\frac{\partial\theta_0}{\partial y},$$

$$\frac{\partial\theta_0}{\partial t} + \frac{\partial\psi_0}{\partial y}\frac{\partial\theta_0}{\partial x} - \frac{\partial\psi_0}{\partial x}\frac{\partial\theta_0}{\partial y} = \nabla^2\theta_0,$$

$$\frac{\partial}{\partial y}\left[(1+\epsilon\theta_{00} - L_2\theta_0))\frac{\partial\varphi_0}{\partial y}\right] = 0.$$

(14)

First-Order System Model

$$\frac{\partial}{\partial t}\nabla^2\psi_1 + \frac{\partial\psi_1}{\partial y}\nabla^2\frac{\partial\psi_0}{\partial x} + \frac{\partial\psi_0}{\partial y}\nabla^2\frac{\partial\psi_1}{\partial x} - \frac{\partial\psi_0}{\partial x}\nabla^2\frac{\partial\psi_1}{\partial y} - \frac{\partial\psi_1}{\partial x}\nabla^2\frac{\partial\psi_0}{\partial y} = \frac{1}{eR_e}\nabla^4\psi_1$$

$$-\frac{1}{R_e}\left(\frac{1}{\sigma} + \frac{M}{1+m^2}\right)\nabla^2\psi_1 + \frac{\gamma}{2}\left[\frac{\partial}{\partial y}\left(\left(\frac{\partial\varphi_0}{\partial y}\right)^2\frac{\partial\theta_1}{\partial x} + 2\frac{\partial\varphi_0}{\partial y}\frac{\partial\varphi_1}{\partial y}\frac{\partial\theta_0}{\partial x}\right) - \frac{\partial}{\partial x}\left(\left(\frac{\partial\varphi_0}{\partial y}\right)^2\frac{\partial\theta_1}{\partial y} + 2\frac{\partial\varphi_0}{\partial y}\frac{\partial\varphi_1}{\partial y}\frac{\partial\theta_0}{\partial y}\right)\right],$$

$$\frac{\partial\theta_1}{\partial t} + \frac{\partial\psi_0}{\partial y}\frac{\partial\theta_1}{\partial x} + \frac{\partial\psi_1}{\partial y}\frac{\partial\theta_0}{\partial x} - \frac{\partial\psi_0}{\partial x}\frac{\partial\theta_1}{\partial y} - \frac{\partial\psi_1}{\partial x}\frac{\partial\theta_0}{\partial y} = \nabla^2\theta_1,\quad \frac{\partial}{\partial y}\left[(1+\epsilon\theta_{00} - L_2\theta_0))\frac{\partial\varphi_1}{\partial y} - L_2\theta_1\frac{\partial\varphi_0}{\partial y}\right] = 0.$$

(15)

Second-Order System Model

$$\frac{\partial}{\partial t}\nabla^2\psi_2 + \frac{\partial\psi_0}{\partial y}\nabla^2\frac{\partial\psi_2}{\partial x} + \frac{\partial\psi_1}{\partial y}\nabla^2\frac{\partial\psi_1}{\partial x} + \frac{\partial\psi_2}{\partial y}\nabla^2\frac{\partial\psi_0}{\partial x} - \frac{\partial\psi_0}{\partial x}\nabla^2\frac{\partial\psi_2}{\partial y} - \frac{\partial\psi_1}{\partial x}\nabla^2\frac{\partial\psi_1}{\partial y} - \frac{\partial\psi_2}{\partial x}\nabla^2\frac{\partial\psi_0}{\partial y} = \frac{1}{eR_e}\nabla^4\psi_2$$

$$-\frac{1}{R_e}\left(\frac{1}{\sigma} + \frac{M}{1+m^2}\right)\nabla^2\psi_2 + \frac{\gamma}{2}\left[\frac{\partial}{\partial y}\left(\left(\frac{\partial\varphi_0}{\partial y}\right)^2\frac{\partial\theta_2}{\partial x} + \left(\frac{\partial\varphi_1}{\partial y}\right)^2\frac{\partial\theta_0}{\partial x} + 2\frac{\partial\varphi_0}{\partial y}\frac{\partial\varphi_1}{\partial y}\frac{\partial\theta_1}{\partial x} + 2\frac{\partial\varphi_0}{\partial y}\frac{\partial\varphi_2}{\partial y}\frac{\partial\theta_0}{\partial x}\right)\right.$$

$$\left.-\frac{\partial}{\partial x}\left(\left(\frac{\partial\varphi_0}{\partial y}\right)^2\frac{\partial\theta_2}{\partial y} + \left(\frac{\partial\varphi_1}{\partial y}\right)^2\frac{\partial\theta_0}{\partial y} + 2\frac{\partial\varphi_0}{\partial y}\frac{\partial\varphi_1}{\partial y}\frac{\partial\theta_1}{\partial y} + 2\frac{\partial\varphi_0}{\partial y}\frac{\partial\varphi_2}{\partial y}\frac{\partial\theta_0}{\partial y}\right)\right],$$

$$\frac{\partial\theta_2}{\partial t} + \frac{\partial\psi_0}{\partial y}\frac{\partial\theta_2}{\partial x} + \frac{\partial\psi_1}{\partial y}\frac{\partial\theta_1}{\partial x} + \frac{\partial\psi_2}{\partial y}\frac{\partial\theta_0}{\partial x} - \frac{\partial\psi_0}{\partial x}\frac{\partial\theta_2}{\partial y} - \frac{\partial\psi_1}{\partial x}\frac{\partial\theta_1}{\partial y} - \frac{\partial\psi_2}{\partial x}\frac{\partial\theta_0}{\partial y} = \nabla^2\theta_2,$$

$$\frac{\partial}{\partial y}\left((1+\epsilon\theta_{00} - L_2\theta_0)\frac{\partial\varphi_2}{\partial y} - L_2\theta_1\frac{\partial\varphi_1}{\partial y} - L_2\theta_2\frac{\partial\varphi_0}{\partial y}\right) = 0.$$

(16)

Zero Order Solution At this order, we have the case of free pumping which means that the fluid is stationary. The solution will take the form

$$u_0 = 0 \quad , \quad v_0 = 0,$$
$$\theta_0(y) = -y + \frac{\theta_{00}+\theta_{10}}{2\beta d},$$
$$\varphi_0(y) = -\frac{a_1}{L_2}\ln(h+L_2 y),$$
$$p_0^*(y) = \frac{\gamma a_1^2}{2L_2[h+L_2 y]} + b_0, \tag{17}$$

where b_0 is arbitrary constant, $a_1 = \frac{\varphi_{10}L_2}{E_0 d \ln(1+2L_2)}$ is the electric parameter and $h = 1 + L_2$.

First Order Solution From Eq. 17 in Eq. 15, we find,

$$\frac{\partial}{\partial t}\nabla^2 \psi_1 = \frac{1}{eR_e}\nabla^4 \psi_1 - \frac{1}{R_e}\left(\frac{1}{\sigma} + \frac{M}{1+m^2}\right)\nabla^2\psi_1$$
$$+ \frac{\gamma}{2}\left(\frac{\partial}{\partial y}\left(\frac{\partial\varphi_0}{\partial y}\right)^2\frac{\partial\theta_1}{\partial x} - 2\frac{\partial\varphi_0}{\partial y}\frac{\partial^2\varphi_1}{\partial x\partial y}\frac{\partial\theta_0}{\partial y}\right), \frac{\partial\theta_1}{\partial t} = \nabla^2\theta_1,$$
$$\frac{\partial}{\partial y}\left((1+\epsilon\theta_{00} - L_2\theta_0)\frac{\partial\varphi_1}{\partial y} - L_2\theta_1\frac{\partial\varphi_0}{\partial y}\right) = 0. \tag{18}$$

Equation 18 can be satisfied in the form

$$\psi_1 = \frac{1}{2}F_1(y)\exp[i\alpha_0(x-t)] + C.C.,$$
$$\varphi_1 = \frac{1}{2}E_1(y)\exp[i\alpha_0(x-t)] + C.C.,$$
$$\theta_1 = \frac{1}{2}T_1(y)\exp[i\alpha_0(x-t)] + C.C.. \tag{19}$$

where the C.C. denotes the complex conjugate. Then, from Eq. 19 in Eq. 18 we get,

$$\frac{1}{e}\frac{d^4 F_1(y)}{dy^4} + \left(\frac{-2\alpha_0^2}{e} + i\alpha_0 R_e - \left(\frac{1}{\sigma} + \frac{M}{1+m^2}\right)\right)\frac{d^2 F_1(y)}{dy^2}$$
$$+ \left(-i\alpha_0^3 R_e + \frac{\alpha_0^4}{e} + \alpha_0^2\left(\frac{1}{\sigma} + \frac{M}{1+m^2}\right)\right)F_1(y)$$
$$- \frac{iR_e\alpha_0 L_2 a_1^{\,2}\gamma}{(h+L_2 y)^3}T_1(y) - \frac{iR_e\alpha_0 a_1\gamma}{(h+L_2 y)}\frac{dE_1(y)}{dy} = 0,$$
$$\frac{d^2 T_1(y)}{dy^2} + \left(i\alpha_0 - \alpha_0^2\right)T_1(y) - i\alpha F_1(y) = 0,$$
$$\frac{d}{dy}\left((h+L_2 y)\frac{dE_1(y)}{dy} + \frac{a_1 L_2 T_1(y)}{(h+L_2 y)}\right) = 0, \tag{20}$$

with the boundary conditions

$$\frac{dF_1}{dy}(\pm 1) = 0 \ , \ F_1 = \pm 1 \ , \ T_1(\pm 1) = \pm 1,$$
$$E_1 = -a_1 \ , \ E_1 = \frac{a_1}{1+2L_2}. \tag{21}$$

The system of Eqs. 20 and 21 has a solution in terms of the wave number α_0 in the form

$$F_1(y) = F_{10}(y) + \alpha_0 F_{11}(y) + ...,$$
$$T_1(y) = T_{10}(y) + \alpha_0 T_{11}(y) + ...,$$
$$E_1(y) = E_{10}(y) + \alpha_0 E_{11}(y) + ... \tag{22}$$

Substituting Eq. 22 into Eqs. 20 and 21 and collecting once again terms of like powers of α_0, we obtain

α_0 - Zero Order

$$\frac{1}{e}\frac{d^4 F_{10}}{dy^4} - \tau\frac{d^2 F_{10}}{dy^2} = 0,$$
$$\frac{d^2 T_{10}}{dy^2} = 0,$$
$$\frac{d}{dy}\left((h+L_2 y)\frac{dE_{10}(y)}{dy} + \frac{a_1 L_2 T_{10}(y)}{(h+L_2 y)}\right) = 0, \tag{23}$$

with the corresponding boundary conditions:

$$\frac{dF_{10}}{dy}(\pm 1) = 0 \ , \ F_{10}(\pm 1) = 0,$$
$$T_{10}(\pm 1) = \pm 1,$$
$$E_{10}(-1) = -a_1 \ , \ E_{10}(1) = \frac{a_1}{1+2L_2}. \tag{24}$$

Where $\tau = \frac{1}{\sigma} + \frac{M}{1+m^2}$.

α_0 - First Order

$$\frac{1}{e}\frac{d^4 F_{11}}{dy^4} - \tau\frac{d^2 F_{11}}{dy^2} = -iR_e\frac{d^2 F_{10}(y)}{dy^2}$$
$$+ \frac{iR_e L_2 a_1^{\,2}\gamma}{(h+L_2 y)^3}T_{10}(y) + \frac{iR_e a_1\gamma}{(h+L_2 y)}\frac{dE_{01}(y)}{dy},$$

$$\frac{d^2 T_{11}}{dy^2} = -i(T_{10}(y) - F_{10}(y)),$$
$$\frac{d}{dy}\left((h+L_2 y)\frac{dE_{11}(y)}{dy} + \frac{a_1 L_2 T_{11}(y)}{(h+L_2 y)}\right) = 0, \tag{25}$$

with the corresponding boundary conditions:

$$\frac{dF_{11}}{dy}(\pm 1) = 0 \ , \ F_{11}(\pm 1) = 0,$$
$$T_{11}(\pm 1) = 0,$$
$$E_{11}(\pm 1) = 0. \tag{26}$$

α_0 - Zero Order Solution Equation 23 solved using the boundary conditions (24) in the form,

$$F_{10}(y) = \frac{-y\sqrt{e\tau}\cosh(\sqrt{e\tau}) + \sinh(y\sqrt{e\tau})}{-\sqrt{e\tau}\cosh(\sqrt{e\tau}) + \sinh(\sqrt{e\tau})},$$
$$T_{10}(y) = y,$$
$$E_{10} = \frac{a_1 y}{h+L_2 y}. \tag{27}$$

α_0 - First Order Solution Using the boundary conditions (26)
the Eq. 25 can be solved in the form,

$$F_{11}(y) = c_1 \cosh(\sqrt{e\tau}\, y) + c_2 \sinh(e\sqrt{\tau}\, y) + c_3 y + c_4 + g(y),$$

$$T_{11}(y) = \frac{i\left(y\left(6 + (-1 + y^2)\, e\tau\right) \sinh(\sqrt{e\tau}) - 6\sinh(\sqrt{e\tau}\, y)\right)}{6(e\tau)^{3/2} \cosh(\sqrt{e\tau}) - 6\tau \cosh(\sqrt{e\tau}\, y)},$$

$$E_{11}(y) = \frac{1}{360 h^4 L_2 e^{5/2} \tau^{5/2}\left(\sqrt{e\tau}\cosh(\sqrt{e\tau}) - \sinh(\sqrt{e\tau})\right)} (iaL_2^2(360(h^2 e\tau - 2hL_2 e\tau y + 3L_2^2(2 +$$

$$y^2 e\tau))\cosh(\sqrt{e\tau}\, y) + \sqrt{e\tau}(e\tau y^2(-15L_2^2 y^2\left(18 - 3e\tau + 2y^2 e\tau\right) + 8hL_2 y\left(30 - 5e\tau + 3y^2 e\tau\right)$$

$$-15h^2\left(12 + (-2 + y^2)\, e\tau\right))\sinh(\sqrt{e\tau}) + 720L_2(h - 3L_2 y)\sinh(y\sqrt{e\tau}))) + 360 h^4 (e\tau)^{5/2}$$

$$\ln(h + L_2 y)\left(\sqrt{e\tau}\cosh\left(\sqrt{e\tau}\right) - \sinh\left(\sqrt{e\tau}\right)\right) c_5) + c_6, \tag{28}$$

where,

$$g(y) = \frac{iR\left(2\sqrt{e}\sqrt{\tau}\, y \cosh\left(\sqrt{e}\sqrt{\tau}\, y\right) - \sinh\left(\sqrt{e}\sqrt{\tau}\, y\right)\right)}{4\tau\left(\sqrt{e}\sqrt{\tau}\cosh\left(\sqrt{e}\sqrt{\tau}\right) - \sinh\left(\sqrt{e}\sqrt{\tau}\right)\right)} + \frac{ia^2\gamma R}{60 e^2 h^7 \tau^3}(30 e h^3 \tau\left(e\tau y^2 + 2\right) -$$

$$20 e h^2 L_2 \tau y\left(e\tau y^2 + 6\right) + 15 h L_2^2\left(e\tau y^2\left(e\tau y^2 + 12\right) + 24\right) - 12 L_2^3 y\left(e\tau y^2\left(e\tau y^2 + 20\right) + 120\right)). \tag{29}$$

The second order solution of our needed system of a_0 can
be obtained by substituting Eqs.(17) in Eqs. (16), we find

$$\frac{\partial}{\partial t}\nabla^2\psi_2 + \frac{\partial\psi_1}{\partial y}\nabla^2\frac{\partial\psi_1}{\partial x} - \frac{\partial\psi_1}{\partial x}\nabla^2\frac{\partial\psi_1}{\partial y} = \frac{1}{eR_e}\nabla^4\psi_2 - \frac{1}{R_e}\left(\frac{1}{\sigma} + \frac{M}{1 + m^2}\right)\nabla^2\psi_2 + \frac{\gamma}{2}\left[\frac{\partial}{\partial y}\right.$$

$$\left(\left(\frac{\partial\varphi_0}{\partial y}\right)^2\frac{\partial\theta_2}{\partial x} + 2\frac{\partial\varphi_0}{\partial y}\frac{\partial\varphi_1}{\partial y}\frac{\partial\theta_1}{\partial x}\right) - \frac{\partial}{\partial x}\left(\left(\frac{\partial\varphi_0}{\partial y}\right)^2\frac{\partial\theta_2}{\partial y} + \left(\frac{\partial\varphi_1}{\partial y}\right)^2\frac{\partial\theta_0}{\partial y} + 2\frac{\partial\varphi_0}{\partial y}\frac{\partial\varphi_1}{\partial y}\frac{\partial\theta_1}{\partial y} + 2\frac{\partial\varphi_0}{\partial y}\frac{\partial\varphi_2}{\partial y}\frac{\partial\theta_0}{\partial y}\right)\right],$$

$$\frac{\partial\theta_2}{\partial t} + \frac{\partial\psi_1}{\partial y}\frac{\partial\theta_1}{\partial x} - \frac{\partial\psi_1}{\partial x}\frac{\partial\theta_1}{\partial y} = \nabla^2\theta_2, \quad \frac{\partial}{\partial y}\left((1 + \epsilon\theta_{00} - L_2\theta_0)\frac{\partial\varphi_2}{\partial y} - L_2\theta_1\frac{\partial\varphi_1}{\partial y} - L_2\theta_2\frac{\partial\varphi_0}{\partial y}\right) = 0. \tag{30}$$

Equation 30 can be satisfied by a solution of the form

$$\psi_2 = \frac{1}{2}\left(F_{20}(y) + F_2(y)\exp\left[i\alpha_0(x - t)\right] + C.C.\right),$$

$$\varphi_2 = \frac{1}{2}\left(E_{20}(y) + E_2(y)\exp\left[i\alpha_0(x - t)\right] + C.C.\right),$$

$$\theta_2 = \frac{1}{2}\left(T_{20}(y) + T_2(y)\exp\left[i\alpha_0(x - t)\right] + C.C.\right). \tag{31}$$

Then, we get the steady part F_{20} in the form

$$\frac{1}{e}\frac{d^3 F_{20}}{dy^3} - \tau\frac{dF_{20}}{dy} = \frac{iR_e\alpha_0}{2}\left[-F_1\frac{d^2 F_1{}^*}{dy^2} + F_1{}^*\frac{d^2 F_1}{dy^2} + \frac{a_1\gamma}{h + L_2 y}\left(T_1\frac{d^2 E_1{}^*}{dy^2} - T_1{}^*\frac{d^2 E_1}{dy^2}\right)\right] + 2c_{20}, \quad \frac{d^2 T_{20}}{dy^2}$$

$$= \frac{i\alpha_0}{2}\left(\frac{dF_1{}^*}{dy}T_1 - \frac{dF_1}{dy}T_1{}^* - \frac{dT_1{}^*}{dy}F_1 + \frac{dT_1}{dy}F_1{}^*\right), \quad \frac{d}{dt}\left[(h + L_2 y)\frac{dE_{20}}{dy}\right.$$

$$\left. -\frac{L_2}{2}\left(\frac{dE_1}{dy}T_1{}^* + \frac{dE_1{}^*}{dy}T_1\right) + \frac{a_1 L_2 T_{20}}{h + L_2 y}\right] = 0, \tag{32}$$

with boundary conditions

$$\frac{dF_{20}}{dy}(\pm) = \mp \frac{1}{2}\left(\frac{d^2F_1}{dy^2}(\pm) + \frac{d^2F_1^*}{dy^2}(\pm)\right) = D,$$

$$T_{20}(\pm) = \mp \frac{1}{2}\left(\frac{dT_1}{dy}(\pm) + \frac{dT_1^*}{dy}(\pm)\right),$$

$$E_{20}(-1) = -\frac{a_1 L_2}{2} + \frac{1}{2}\left(\frac{dE_{-1}}{dy}(-1) + \frac{dE_1^*}{dy}(-1)\right),$$

$$E_{20}(1) = -\frac{a_1 L_2}{2(h+L_2)} - \frac{1}{2}\left(\frac{dE_1}{dy}(1) + \frac{dE_1^*}{dy}(1)\right). \quad (33)$$

From the Eqs. 28, 27 and using the boundary conditions (33) in (32), the system equations of (32) can be easily solved in the form

$$F_{20}'(y) = -\frac{2c_{20}}{e\tau}\left(1 - \frac{\cosh(\sqrt{e\tau}y)}{\cosh(\sqrt{e\tau})}\right) + \frac{(\tau(2D-k(-1)-k(1)))}{2\tau}\frac{\cosh(\sqrt{e\tau}y)}{\cosh(\sqrt{e\tau})}$$
$$+ \frac{(k(-1)-k(1))}{2}\frac{\sinh(\sqrt{e\tau}y)}{\sinh(\sqrt{e\tau})} + k(y). \quad (34)$$

Where $D = \frac{e\tau}{\sqrt{e}\sqrt{\tau}\coth(\sqrt{e}\sqrt{\tau})-1}$

$$T_{20}(y) = n(y) + c_9 y + c_{10},$$

$$E_{20}(y) = w(y) + c_{11}\ln(h+L_2 y) + c_{12}.$$

Thus, the mean time-averaged velocity is

$$\bar{u}(y) = \frac{1}{2\pi}\int_0^{2\pi} u(y,t)dt = u_0(y) + \frac{a_0^2}{2}F_{20}'(y), \quad (35)$$

the mean time-averaged heat is

$$\overline{T}(y) = \frac{1}{2\pi}\int_0^{2\pi} T(y,t)dt = \theta_0(y) + \frac{a_0^2}{2}T_{20}'(y), \quad (36)$$

and the mean time-averaged electric potential is

$$\overline{\varphi}(y) = \frac{1}{2\pi}\int_0^{2\pi} \varphi(y,t)dt = \varphi_0(y) + \frac{a_0^2}{2}E_{20}'(y). \quad (37)$$

From the Eqs. 13, 17, 19 and 22 in the Eq. 11, and each term is averaged over an interval of time. then the second order mean pressure gradient may given as

$$\overline{\frac{\partial p_2}{\partial x}} = \frac{1}{2rR_e}\frac{d^3F_{20}}{dy^3} - \frac{\tau}{2R_e}\frac{dF_{20}}{dy} + \frac{iR\alpha_0}{4}\left[F_1\frac{d^2F_1^*}{dy^2} - F_1^*\frac{d^2F_1}{dy^2}\right]$$
$$- \frac{a_1\gamma}{h+L_2 y}\left(T_1\frac{dE_1^*}{dy} - T_1^*\frac{dE_1}{dy}\right)\right] = \frac{C_{20}}{eR_e}. \quad (38)$$

Then its find that the constant c_{20} is proportional with the mean pressure gradient $\overline{\frac{\partial p_2}{\partial x}}$. From Eqs. 34, 35 and 38, the mean-time average velocity can be written as,

$$\bar{u}(y) = \frac{a_0^2}{2}\left(-2\frac{R_e}{\tau}\overline{\frac{\partial p_2}{\partial x}}\left(1 - \frac{\cosh(\sqrt{e\tau}y)}{\cosh(\sqrt{e\tau})}\right)\right.$$
$$+ \frac{(\tau(2D-k(-1)-k(1)))}{2\tau}\frac{\cosh(\sqrt{e\tau}y)}{\cosh(\sqrt{e\tau})}$$
$$\left. + \frac{(k(-1)-k(1))}{2}\frac{\sinh(\sqrt{e\tau}y)}{\sinh(\sqrt{e\tau})} + k(y)\right). \quad (39)$$

If we neglect the external body force effects and the effect of magnetic field in Eq. 9 we get the same solution of [30] in absence the slip condition as

$$\bar{u}(y) = \frac{a_0^2}{2}\left(-2\sigma R_e\overline{\frac{\partial p_2}{\partial x}}\left(1 - \frac{\cosh(\sqrt{\frac{e}{\sigma}}y)}{\cosh(\sqrt{\frac{e}{\sigma}})}\right)\right.$$
$$\left. + (D-k(1))\frac{\cosh\left(\sqrt{\frac{e}{\sigma}}y\right)}{\cosh\left(\sqrt{\frac{e}{\sigma}}\right)} + k(y)\right). \quad (40)$$

4 Comparison with Theoretical Results

We comprise our analytical solution with the theoretical results that obtained by Fung and Yih [29] and Maiti and Misra [30]:

- When $M \to 0$ and $L \to 0$, our numerical results are the same of those obtained by Maiti and Misra [30].
- When $M \to 0$, $L \to 0$ and $\sigma \to \infty$, our numerical results are the same of those obtained by Fung and Yih [29].

as shown in the Fig. 2

5 Results and Discussion

In the problem solution, we have shown the analytical expressions of the mean time-averaged velocity, the mean time-averaged temperature, and the mean time-averaged electric potential.
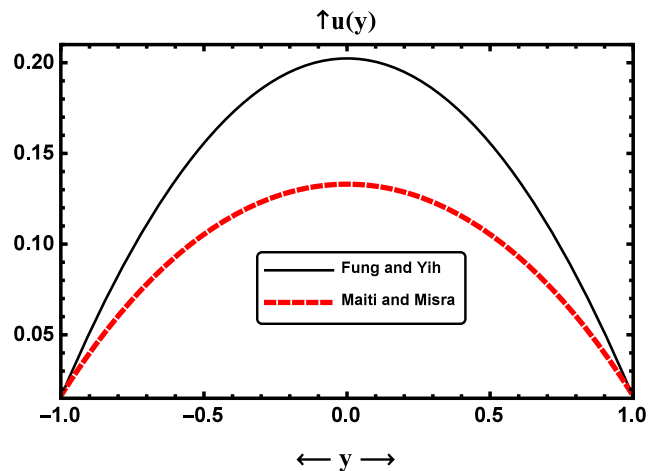
Fig. 2 Comparison between analytical solution and the theoretical results that obtained by Fung and Yih [29] and Maiti and Misra [30] on the mean time-averaged velocity $\bar{u}(y)$ at $R_e = 15$, $\sigma = 1$, $e = 0.9$, $a_0 = 0.1$ and $\alpha_0 = 0.25$
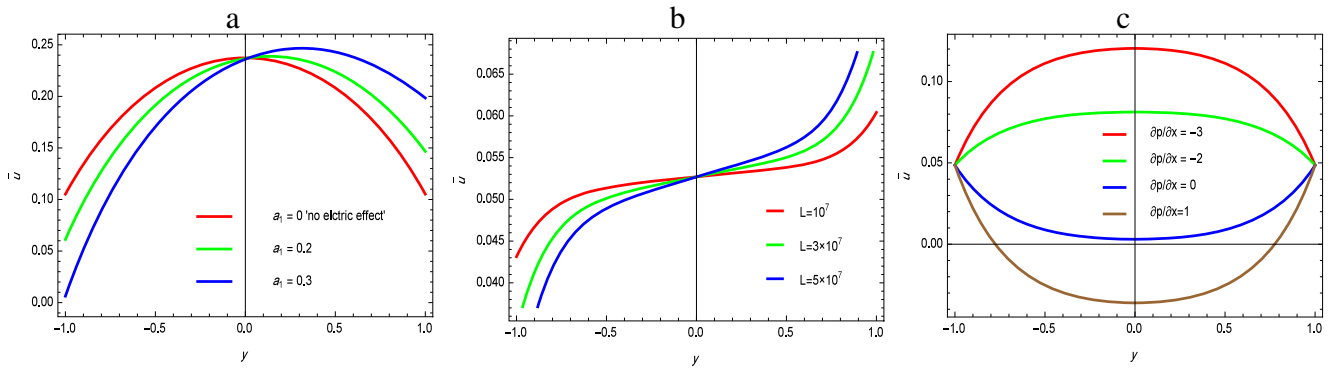
Fig. 3 **a** Effect of the parameter a_1 on the distribution of the mean velocity for $R_e = 50$, $L_2 = 0.02$, $M = 2$, $m = 0.1$, $\sigma = 0.1$, $a_0 = 0.1$, $e = 0.7$, $\alpha_0 = 0.01$, $\frac{\partial p_2}{\partial x} = -3$, and $L = 10000$. **b** Effect of the electrical Rayleigh number on the distribution of the mean velocity for $R_e = 50$, $L = 0.01$, $M = 10$, $m = 0.1$, $\sigma = 0.9$, $a_1 = 0.02$, $e = 0.7$, $a_0 = 0.1$, $\alpha_0 = 0.01$ and $\frac{\partial p_2}{\partial x} = -3$. **c** Effect of the pressure gradient on the distribution of the mean velocity for $R_e = 50$, $L = 10000$, $L_2 = 0.1$, $M = 2$, $m = 0.1$, $\sigma = 0.1$, $a_1 = 0.001$, $e = 1$, $a_0 = 0.1$ and $\alpha_0 = 0.01$

Generally, Fung and Yih applied the peristaltic transport during the ureter theoretically [29] and experimentally by Yin and Fung [31].

- In the theoretical study [29], the peristaltic transport for the ureter was simulated by using the following parameters as $R_e : 0 \to 100$ and $\alpha_0 : 0.05 \to 0.4$.
- In the experimental study [31], the ureter parameters are taken as ureter length $= 81.28\,cm$, $\lambda = 9.8\,cm$, $a = 0.256\,cm$, $d = 0.635\,cm$, and $\alpha = 3.77\,cm$. In the dimensionless quantities the parameters become $a_0 = 0.41$, $\alpha_0 = 0.385$, and $R_e : 0.5 \to 2.5$.

Accordingly, we used the values of dimensionless parameters based on the theoretical and experimental studies to investigate our problem as $a_0 = 0.1$, $\alpha_0 : 0 \to 0.9$, $R_e : 0.5 \to 100$, $M > \sqrt{2}$ [17–24], and $L > 10000$ [3–5], which agree with the previous experimental and theoretical studies by others.

The discussion section is divided into three subsections. In the first subsection, the effects of the various parameters are discussed on the mean time-averaged velocity. In the second subsection, we discuss the effects of the various parameters on the mean time-averaged temperature and the mean time-averaged electric potential. Moreover, the critical pressure gradient for reflux is illustrated in the third subsection.

5.1 Mean Time-Averaged Velocity

Numerical computation based on Eq. 39 detects that the averaged axial velocity distribution for EHD fluid induced by sinusoidal wavy walls through a porous medium with heat transfer is dominated by the constant $\frac{D}{\cosh(\sqrt{e\tau})}$ and the parabolic distribution $2\frac{R_e}{\tau}\overline{\frac{\partial p_2}{\partial x}}\left(1 - \frac{\cosh(\sqrt{e\tau}y)}{\cosh(\sqrt{e\tau})}\right)$ in addition to three terms $k(y) + \frac{(k(-1)-k(1))}{2}\frac{\sinh(\sqrt{e\tau}y)}{\sinh(\sqrt{e\tau})} -$
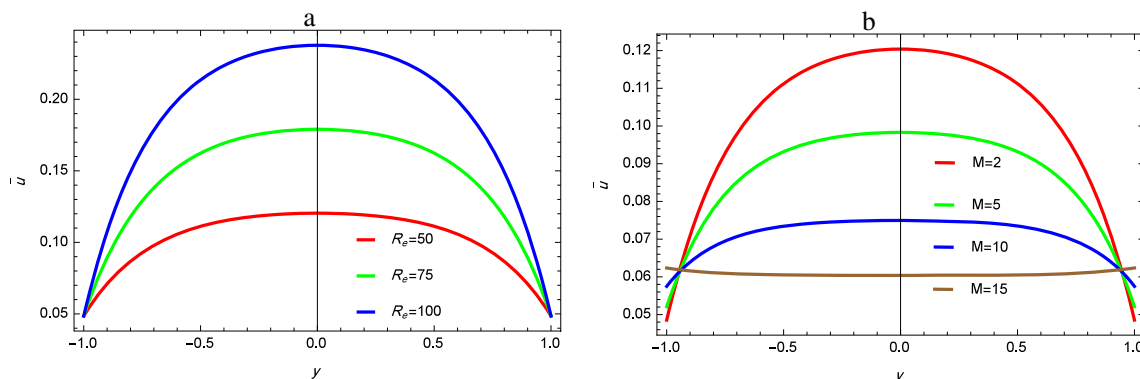
Fig. 4 **a** Effect of the Reynolds number on the distribution of the mean velocity for $L = 10000$, $e = 1$, $L_2 = 0.1$, $M = 2$, $m = 0.1$, $\sigma = 0.1$, $a_1 = 0.001$, $a_0 = 0.1$, $\alpha_0 = 0.01$ and $\frac{\partial p_2}{\partial x} = -3$. **b** Effect of the magnetic field on the distribution of the mean velocity for $L = 10000$, $L_2 = 0.01$, $e = 1$, $R_e = 50$, $m = 0.1$, $\sigma = 0.1$, $a_1 = 0.001$, $a_0 = 0.1$, $\alpha_0 = 0.01$ and $\frac{\partial p_2}{\partial x} = -3$
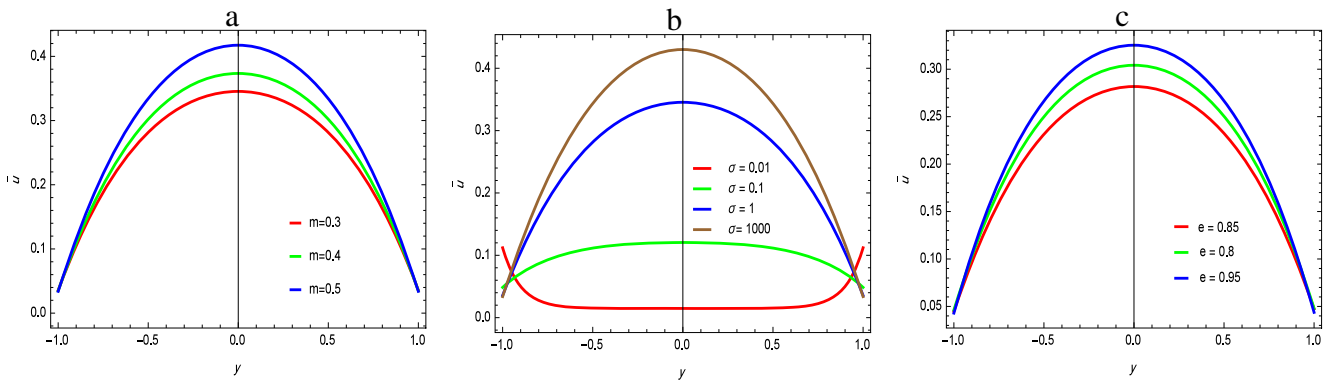
Fig. 5 **a** Effect of the the Hall parameter on the distribution of the mean velocity for $L = 10000$, $L_2 = 0.01$, $e = 1$, $R_e = 50$, $M = 2$, $\sigma = 1$, $a_1 = 0.001$, $a_0 = 0.1$, $\alpha_0 = 0.5$ and $\frac{\partial p_2}{\partial x} = -3$. **b** Effect of the permeability parameter on the distribution of the mean velocity for $L = 10000$, $L_2 = 0.01$, $R_e = 50$, $M = 2$, $m = 0.1$, $a_1 = 0.001$, $a_0 = 0.1$, $\alpha_0 = 0.5$, $e = 1$ and $\frac{\partial p_2}{\partial x} = -3$. **c** Effect of the porosity parameter on the distribution of the mean velocity for $L = 10000$, $L_2 = 0.1$, $R_e = 15$, $\sigma = 1$, $M = 2$, $m = 0.1$, $a_1 = 0.001$, $a_0 = 0.1$, $\alpha_0 = 0.5$ and $\frac{\partial p_2}{\partial x} = -3$

$\frac{(\tau(k(-1)+k(1)))}{2\tau}\frac{\cosh(\sqrt{e\tau}\,y)}{\cosh(\sqrt{e\tau})}$ that represents the perturbation of the velocity across the channel.

The constant D, which defines the velocity boundary value of F'_{20}, depends on magnetic field M, Hall parameter m, porosity parameter e and permeability parameter σ and appears from the expression of the radial gradient of the first-order axial velocity distribution as shown in Eq. 33.

Figures 3, 4, and 5 illustrate the effect of the different parameters on the mean velocity $\overline{u}(y)$. Figure 3a shows that in the absence of the electric field, i.e., electric parameter $a_1 = 0$, the behavior of the mean velocity $\overline{u}(y)$ will be symmetric and by increasing the value of electric parameter a_1, the behavior becomes asymmetric. Also, we find that the velocity increases near the upper bound but decreases near the lower bound of the channel. This occurs according to the boundary conditions of the electric potential $\varphi(y)$. Interpretation physicist, the existence of the electric field

at the upper bound ($\varphi \neq 0$) decreases the density of the fluid which making the fluid molecules freely moving, and this leads to increase in the fluid velocity. When the value of electric parameter $a_1 \neq 0$, the effect of the electrical Rayleigh number L will be appear and giving the same effect as a_1 (see Fig. 3b). Figure 3c shows the variant of $\overline{u}(y)$ vs y for different values of the pressure gradient $\frac{\partial p_2}{\partial x}$ and we can see that as $\frac{\partial p_2}{\partial x}$ increases, a reflux flow (back flow) will be appear.

Figure 4a studies the effect of Reynolds number on the distribution of the mean velocity $\overline{u}(y)$ and as expected it is found that the increases of the Reynolds number increase the mean velocity $\overline{u}(y)$. This happens because the Reynolds number is inversely proportional to the viscosity of the fluid. That is, increasing the Reynolds number reduces the viscosity of the fluid, which causes an increase in the velocity of the fluid as expected. Figure 4b illustrates that
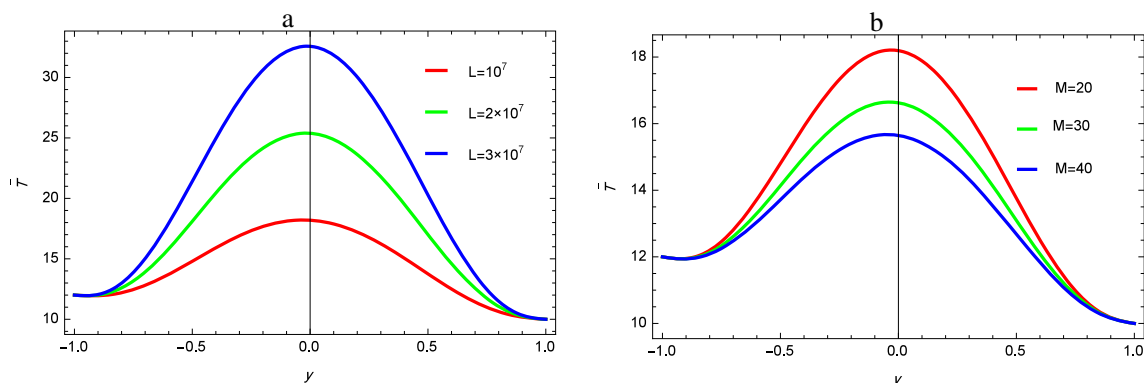
Fig. 6 **a** Effect of the Rayleigh number on the distribution of the mean temperature for $R_e = 100$, $L_2 = 0.1$, $m = 0.1$, $M = 20$, $a_1 = 0.2$, $a_0 = 0.1$, $\sigma = 2$ and $\alpha_0 = 0.9$. **b** Effect of the magnetic field on the distribution of the mean temperature for $R_e = 100$, $L = 0.1$, $m = 0.1$, $L_2 = 10^7$, $a_1 = 0.1$, $a_0 = 0.1$, $\sigma = 2$ and $\alpha_0 = 0.9$
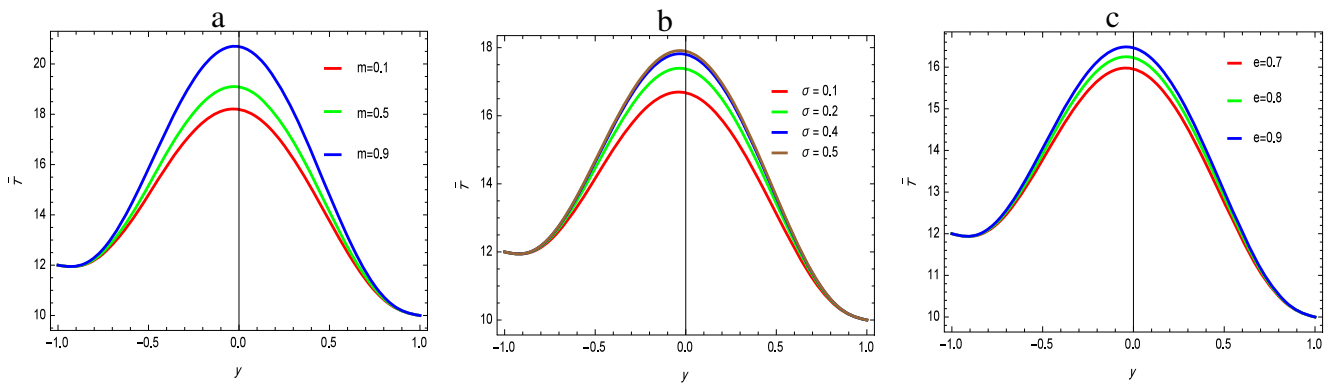
Fig. 7 **a** Effect of the Hall parameter on the distribution of the mean temperature for $R_e = 100$, $L = 0.1$, $M = 20$, $L_2 = 10^7$, $a_1 = 0.1$, $a_0 = 0.1$, $\sigma = 2$ and $\alpha_0 = 0.9$. **b** Effect of the permeability parameter on the distribution of the mean temperature for $R_e = 100$, $L_2 = 0.1$, $M = 20$, $L_2 = 10^5$, $a_1 = 0.1$, $a_0 = 0.1$ and $\alpha_0 = 0.9$. **c** Effect of the porosity parameter r on the distribution of the mean temperature for $R_e = 100$, $L = 0.1$, $M = 2$, $\sigma = 0.1$, $L_2 = 10^5$, $a_1 = 0.1$, $a_0 = 0.1$, $m = 0.1$ and $\alpha_0 = 0.9$

as the magnetic field increases, the mean velocity $\overline{u}(y)$ decreases, i.e., as M increases the Hartmann braking also grows which could be thought as an increase of the magnetic viscosity and so the fluid moves as a block with a constant velocity. From Fig. 5, we found that by increasing the Hall parameter m, the permeability parameter σ, and porosity parameter e, the mean velocity $\overline{u}(y)$ increases.

5.2 Mean Time-Averaged Heat and Mean Time-Averaged Electric Potential

Now, we will study the nature of the mean time-averaged temperature $\overline{T}(y)$ through Figs. 6 and 7. Figure 6a, b shows that the increasing of Rayleigh number increases the mean temperature $\overline{T}(y)$, but a reverse effect is observed by increasing the magnetic field. Also the increase of the Hall parameter m, the permeability parameter σ and porosity parameter e produce an increase in the mean temperature $\overline{T}(y)$ (see Fig. 7). It is also noted from Fig. 7b that the temperature $\overline{T}(y)$ becomes steady as the permeability parameter σ increases.

Figures 8, 9, 10, and 11 illustrate the behavior of the mean time-averaged electric potential $\overline{\varphi}(y)$. Figure 8a shows that the greater of the Rayleigh number L increases the mean time-averaged electric potential near the walls but reduces as we moves far from the walls. Figure 8b shows that the increasing of the magnetic parameter M decreases the mean time-averaged electric potential $\overline{\varphi}(y)$ but a reverse effect is observed by increasing the Hall parameter m and the permeability parameter σ (see Fig. 9a, b). Also, we found that the mean time-averaged electric potential $\overline{\varphi}(y)$ becomes steady as increasing the permeability parameter σ. From Fig. 9c, we found that the increasing of the porosity parameter e increases the mean time-averaged electric potential $\overline{\varphi}(y)$ near the walls but an opposite effect appears as we move far a way from the walls.

5.3 Critical Pressure Gradient for Reflux

The study of the critical pressure gradient for reflux is very important because the bacteria and some other materials sometimes moves from the bladder to the kidney or from
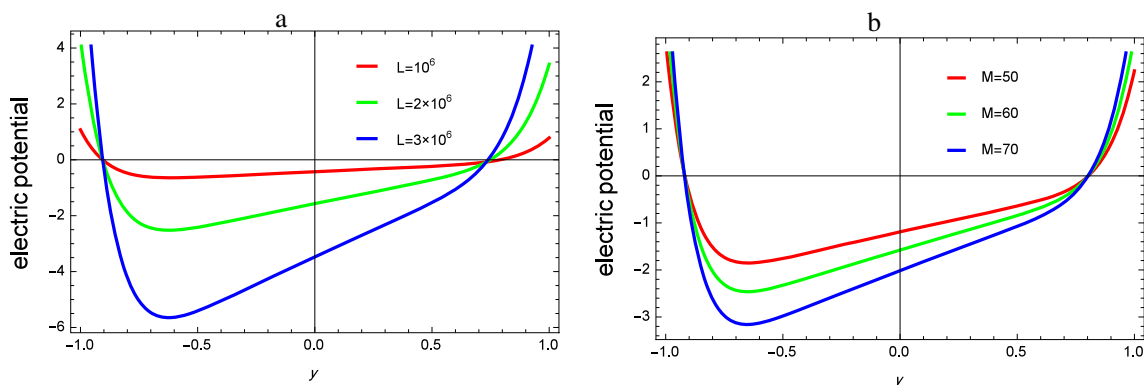
Fig. 8 **a** Effect of the Rayleigh number on the distribution of the mean electric for $R_e = 20$, $L_2 = 0.1$, $m = 0.1$, $M = 2$, $a_1 = 0.05$, $a_0 = 0.1$, $e = 1$, $\sigma = 1$ and $\alpha_0 = 0.1$. **b** Effect of the magnetic field on the distribution of the mean electric for $R_e = 50$, $L_2 = 0.1$, $L = 100000$, $a_1 = 0.05$, $a_0 = 0.1$, $m = 0.1$, $\sigma = 1$, $e = 0.9$, and $\alpha_0 = 0.9$
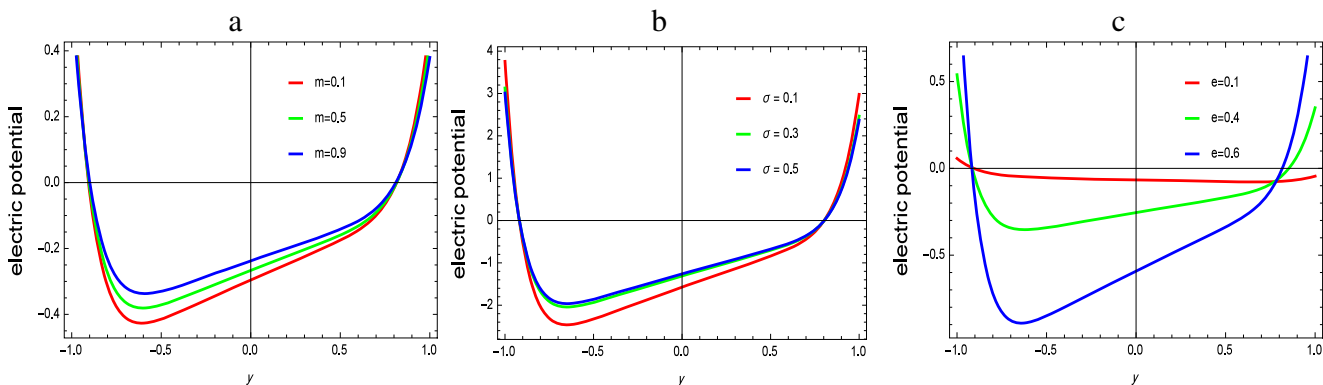
Fig. 9 a Effect of the Hall parameter on the distribution of the mean electric for $R_e = 50$, $L_2 = 0.1$, $L = 100000$, $M = 10$, $a_1 = 0.05$, $a_0 = 0.1$, $e = 0.9$, $\sigma = 1$ and $\alpha_0 = 0.9$. **b** Effect of the permeability parameter on the distribution of the mean electric for $R_e = 50$,

$L_2 = 0.1$, $L = 100000$, $M = 50$, $a_1 = 0.05$, $a_0 = 0.1$, $m = 0.1$, $e = 0.9$ and $\alpha_0 = 0.5$. **c** Effect of porosity parameter on the distribution of the mean electric for $R_e = 50$, $L_2 = 0.1$, $L = 100000$, $M = 50$, $a_1 = 0.05$, $a_0 = 0.1$, $m = 0.1$, $\sigma = 0.1$ and $\alpha_0 = 0.9$

one kidney to the other in the direction opposite to the direction of urine flow. This phenomenon is referred as "ureteral reflux" by physiologists. The riskiness of diseases such as tuberculosis, interstitial cystitis, and duct stone are treated due to this reflux. See Graves and Davidoff [32], Hutch [33], Gruber [34], and Fung and Yih [29].

To get the critical reflux pressure, the value of the mean velocity $\overline{u}(y)$ set to zero in Eq. 39 on the central region at $y = 0$. So, the critical pressure gradient will taken the form,

$$\left(\frac{\partial p_2}{\partial x}\right)_{critical\,pressure} = \frac{\tau}{2R\left(1 - \text{Sech}(\sqrt{e\tau})\right)}\left(k(0) + \frac{1}{2}(2D - k(-1) - k(1))\text{Sech}\left(\sqrt{e\tau}\right)\right).$$

Figures 10 and 11 depict the critical pressure gradient which is plotted against the wave number α_0 that range from $0 - 0.9$. From the behavior of Fig. 10a, we observe that the relation between the critical pressure gradient and wave number α_0 is inversely (the increase of the wave number reduces the critical pressure values), also it is found that the increase of the Reynolds number reduces the critical pressure gradient. Figure 10b shows the effect

of the magnetic field on the critical pressure value, and it can conjectured that the increase of the magnetic field decreases the critical pressure when α_0 is less than 0.38 but a vise versa effect when α_0 more than this value. Figure 11 illustrates the effect of Hall parameter, electric Rayleigh number and porosity parameter respectively and it is found that the increases of the Hall parameter, electric Rayleigh number and porosity parameter decrease the critical pressure value for reflux.

6 Conclusion

In this article, we design a mathematical model describing the electro-magnetohydrodynamic oscillatory flow for a dielectric fluid with heat transfer through a porous medium "Brinkman model." Graphs of the mean average velocity, temperature distribution, and electric potential are drawn for various values of the pressure gradient $\frac{\partial p_2}{\partial x}$, the electric Rayleigh number L, Reynolds number R_e, the magnetic field M, Hall parameter m, porosity parameter e, and
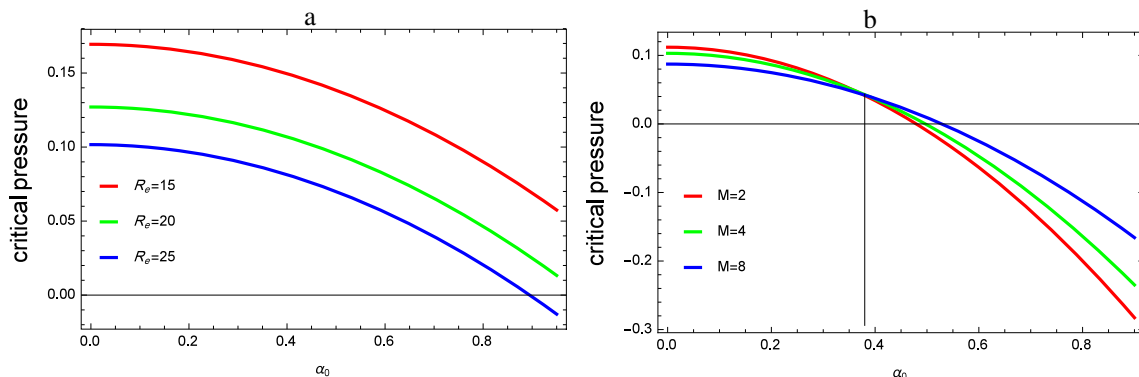
Fig. 10 a Effect of the Reynolds number vs the wave number on the distribution of the critical reflux of pressure for $M = 10$, $L = 100000$, $m = 0.1$, $L_2 = 0.1$, $a_1 = 0.1$, $e = 0.9$ and $\sigma = 0.5$. **b** Effect of

the magnetic field number vs the wave number on the distribution of the critical reflux of pressure for $M = 10$, $L = 1000000$, $m = 0.1$, $L_2 = 0.1$, $R_e = 15$, $a_1 = 0.1$, $e = 0.9$ and $\sigma = 0.05$
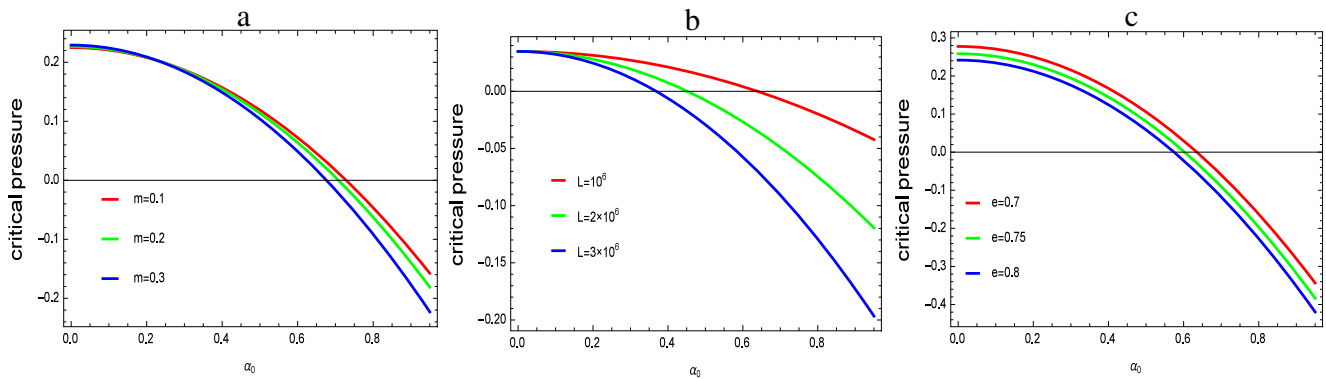
Fig. 11 a Effect of the hall parameter number vs the wave number on the distribution of the critical reflux of pressure for $M = 2$, $L = 100000$, $L_2 = 0.1$, $R_e = 15$, $a_1 = 0.1$, $a_0 = 0.1$, $e = 0.9$ and $\sigma = 0.5$. **b** Effect of the electric Rayleigh number vs the wave number on the distribution of the critical reflux of pressure for $M = 50$, $m = 0.1$, $L_2 = 0.1$, $R_e = 15$, $a_1 = 0.1$, $a_0 = 0.1$, $e = 0.9$ and $\sigma = 0.9$. **c** Effect of the porosity parameter vs the wave number on the distribution of the critical reflux of pressure for $M = 2$, $L = 100000$, $L_2 = 0.1$, $R_e = 15$, $a_1 = 0.1$, $a_0 = 0.1$ and $\sigma = 1000$

the permeability parameter σ. The main outcomes of the present study are concisely summarized as:

- AC electric field accelerates the blood flow velocity and that leads to enhance the blood circulation, which is useful to eliminate the metabolic waste products and endogenous pains producing.
- The electric and magnetic fields have an opposite effect on the mean velocity $\overline{u}(y)$, since the effect of magnetic field is perpendicular to the influence of the electric field.
- The parameter a_1 controls in the electric Raleigh number, in other words the effect of electric Raleigh number exists when $a_1 \neq 0$.
- The mean time average velocity $\overline{u}(y)$ is higher in the presence electric field, where $L \neq 0$, $a_1 \neq 0$

- The second order pressure gradient $\frac{\partial p_2}{\partial x}$ has a significant influence on the reflux mean velocity.
- As the magnetic field increases, the flow moves as a bulk.
- The mean average temperature $\overline{T}(y)$ is greater as the magnetic field decreases and a reverse effect for the Hall and permeability parameters occurs.
- The mean electric potential $\overline{\varphi}(y)$ values is greater as the magnetic field decreases.
- The mean average temperature $\overline{T}(y)$ is greater as the electric parameter a_1 increases.
- The critical reflux pressure value is greater for a fluid without an electric field $L = 0$, $a_1 = 0$.

Appendix

$$h = 1 + L_2,$$

$$c_1 = \frac{\operatorname{csch}\left(\sqrt{e\tau}\right)\left(g'(-1) - g'(1)\right)}{2\sqrt{e\tau}},$$

$$c_2 = -\frac{g(-1) - g(1) + g'(-1) + g'(1)}{2\sqrt{e\tau}\coth(\sqrt{e\tau}) - 2\sinh(\sqrt{e\tau})},$$

$$c_3 = \frac{\sqrt{e\tau}\coth(\sqrt{e\tau})(g(-1) - g(1)) + \sinh(\sqrt{e\tau})g'(-1) + g'(1)}{2\sqrt{e\tau}\coth(\sqrt{e\tau}) - 2\sinh(\sqrt{e\tau})},$$

$$c_4 = \frac{-\sqrt{e\tau}(g(-1) + g(1)) + \coth(\sqrt{e\tau})\left(-g'(-1) + g'(1)\right)}{2\sqrt{e\tau}},$$

$$c_5 = \frac{4ia_1 L_2{}^3\left(45\sqrt{e\tau}\cosh\left(\sqrt{e\tau}\right) + (-45 + (-15 + e\tau)e\tau)\sinh\left(\sqrt{e\tau}\right)\right)}{45\left(1 + L_2\right)^3(e\tau)^2\ln\left(1 + 2L_2\right)\left(\sqrt{e\tau}\cosh\left(\sqrt{e\tau}\right) - \sinh\left(\sqrt{e\tau}\right)\right)},$$

$$c_6 = \frac{ia_1 L_2}{360\left(1 + L_2\right)^4(e\tau)^{5/2}\left(\sqrt{e\tau}\cosh\left(\sqrt{e\tau}\right) - \sinh\left(\sqrt{e\tau}\right)\right)}\Big(360\left(e\tau + 4L_2 e\tau + 6L_2{}^2(1 + e\tau)\right)\cosh(\sqrt{e\tau}) + \sqrt{e\tau}$$

$$\left(-720L_2(1 + 4L_2) - 30\left(6 + L_2(20 + 23L_2)\right)e\tau + (15 + 46L_2(1 + L_2))(e\tau)^2\right)\sinh\left(\sqrt{e\tau}\right)\Big),$$

$$c_7 = \frac{\text{Sech}(\sqrt{e\tau})(\tau(2D - k(-1) - k(1)) + 4ec_{20})}{2e\tau},$$

$$c_8 = 1/2\text{csch}(\sqrt{e\tau})(k(-1) - k(1)),$$

$$c_9 = \frac{1}{2}(n(-1) - n(1)),$$

$$c_{10} = \frac{1}{2}(-n(-1) - n(1)),$$

$$c_{11} = \frac{L_2\left(a(2 - 2L_2(2(L_2 - 2)L_2 + 3)) - (1 - 2L_2)^2(w(-1) - w(1))\right)}{(1 - 2L)^2 \log(1 - 2L_2)},$$

$$c_{12} = \frac{1}{2}a(L_2 - 2) - w(1).$$

References

1. Woodson, H.H., & Melcher, J.R. (1968). *Electromechanical Dynamics*. New York: Massachusetts Institute of Technology.

2. Takashima, M. (1970). The stability of a rotating layer of the Maxwell liquid heated from below. *Journal of the Physical Society of Japan*, *29*, 1061–1068.

3. Takashima, M., & Ghosh, A.K. (1979). Electrohydrodynamic Instability of viscoelastic liquid layer. *Journal of the Physical Society of Japan*, *47*, 1717–1722.

4. Devi, U.V., Puri, P., Sharma, N.N., Ananthasubramanian, M. (2014). Electrokinetics of cells in dielectrophoretic separation: a biological perspective. *BioNanoScience*, *4*, 276–287.

5. El-Sayed, M.F., Harouna, M.H., Mostapha, D.R. (2015). Electro-convection peristaltic flow of viscous dielectric liquid sheet in asymmetrical flexible channel. *Journal of atomization and sprays*, *25*, 985–1011.

6. Srinivasacharya, D., & Rao, G.M. (2017). Modeling of blood flow through a bifurcated artery using nanofluid. *BioNanoScience*, *7*, 1–11.

7. Akbar, V., & Nadeem, S. (2012). Thermal and velocity slip effects on the peristaltic flow a six constant Jeffrey's fluid model. *International Journal of Heat Mass Transfer*, *55*, 3964–3970.

8. Shahzadi, I., Sadaf, H., Nadeem, S., Saleem, A. (2017). Bio-mathematical analysis for the peristaltic flow of single wall carbon nanotubes under the impact of variable viscosity and wall properties. *Computer Methods and Programs in Biomedicine*, *139*, 137–147.

9. Nadeem, S., & Sadaf, H. (2016). Hypothetical analysis for peristaltic transport of metallic nanoparticles in an inclined annulus with variable viscosity. *Bulletin of the Polish Academy of Sciences Technical Sciences*, *64*, 447–454.

10. Hayat, T., Nawaz, S., Alsaadi, A., Rafi, M. (2016). Mixed convective peristaltic flow of water based nanofluids with Joule heating and convective boundary conditions. *PLoS ONE*, *11*, 0153537.

11. Nadeem, S., Mehmood, R., Akbar, N.S. (2012). Non-orthogonal stagnation point flow of a non-Newtonian fluid towards a stretching surface with heat transfer. *International Journal of Heat Mass Transfer*, *55*, 3964–3970.

12. Hina, S., Mustafa, M., Hayat, T., Alsaedi, A. (2015). Peristaltic flow of couple stress fluid with heat and mass transfer: An application in biomedicine. *Journal of Mechanics in Medicine and Biology*, *15*, 1–17.

13. Mekheimer, Kh.S., & Abd elmaboid, Y. (2014). Simultaneous effects of variable viscosity and thermal conductivity on peristaltic flow in a vertical asymmetric channel. *Canadian Journal of Physics*, *92*, 1541–1555.

14. Abd elmaboud, Y., & Mekheimer, Kh.S. (2012). Unsteady pulsatile flow through a vertical constricted annulus with heat transfer. *Verlag der Zeitschrift fur Naturforschung*, *67*, 185–194.

15. Mekheimer, Kh.S., Hasona, W.M., Abo-Elkhair, R.E., Zaher, A.Z. (2018). Peristaltic blood flow with gold nanoparticles as a third grade nano fluid in catheter: application of cancer therapy. *Physics Letters A*, *382*, 85–93.

16. Hayat, T., Noreen, S., Alhothuali, M., Asghar, S., Alhomaidan, A. (2002). Peristaltic flow under the effects of an induced magnetic field and heat and mass transfer. *International Journal of Heat and Mass Transfer*, *55*, 443–452.

17. Abbasi, F.M., Hayat, T., Ahmad, B. (2015). Impact of magnetic field on mixed convective peristaltic flow of water based nanofluids with Joule heating. *Verlag der Zeitschrift fur Naturforschung*, *70*, 125–132.

18. Mekheimer Kh. S., Salem, A.M., Zaher, A.Z. (2014). Peristatc ally induced MHD slip flow in a porous medium due to a surface acoustic wavy wall. *Egyptian Mathematical Society*, *22*, 143–151.

19. Mekheimer, Kh.S., Salem, A.M., Zaher, A.Z. (2013). Peristaltically Induced Flow Due to a Surface Acoustic Wavy Moving Wall. *CHINESE JOURNAL OF PHYSICS*, *51*, 954–968.

20. Abo-Elkhair, R.E., Mekheimer, Kh.S., Moawad, A.M.A. (2018). Combine impacts of electrokinetic variable viscosity and partial slip on peristaltic MHD flow through micro-channel, Iranian Journal of science and tecnology transaction A: science. https://doi.org/10.1007/s40995-017-0374-y.

21. Mekheimer Kh.S. (2008). Effect of induced magnetic field on peristaltic flow of a couple stress Fluid. *Physics Letters A*, *372*, 4271–4278.

22. Mekheimer, Kh.S., Saleem, N., Hayat, T. (2012). Simultaneous effects of induced magnetic field and heat and mass transfer on the peristaltic motion of second-order fluid in a channel. *International Journal for Numerical Methods in Fluids*, *70*, 342–358.

23. Mekheimer Kh.S. (2004). Peristaltic flow of blood under effect of a magnetic field in a non uniform channel. *Applied Mathematics and Computation*, *153*, 763–777.

24. Abo-Elkhair, R.E., Mekheimer, Kh.S., Moawad, A.M.A. (2017). Cilia walls influence on peristaltically induced motion of magneto-fluid through a porous medium at moderate Reynolds number: Numerical Study. *Journal of the Egyptian Mathematical Society*, *25*, 238–251.

25. El Shehawey, E.F., Mekheimer, Kh.S., Kaldas, S.F., Afifi, N.A.S. (1999). Peristaltic transport through a porous medium. *Journal of Biomathematics*, *14*, 1–13.

26. El Shehawey, E.F., Sobh, A.M.F., Elbarbary, E.M.E. (2000). Peristaltic motion of a generalized Newtonian fluid through a porous medium. *Journal of the Physical Society of Japan*, *69*, 401–407.

27. Harris, S.D., Ingham, D.B., Pop, I. (2009). Mixed convection boundary-layer flow near the stagnation point on a vertical surface in a porous medium: Brinkman model with slip. *Transport in Porous Medium*, *77*, 267–285.

28. Wolfgangand, K.H. (1955). *and Phillips A.M.* Cambridge: Addison-Wesley.

29. Fung, Y.C., & Yih, C.S. (1968). Peristaltic transport. *Journal of Applied Mechanics*, *35*, 669–675.

30. Maiti, S., & Misra, J.C. (2011). Peristaltic flow of a fluid in a porous channel: a study having relevance to flow of bile within ducts in a pathological state. *International Journal of Engineering Science*, *9*, 950–966.

31. Yin, F.C.P., & Fung, Y.C. (1971). Comparison of theory and experimen in peristaltic transport. *J. Fluid Mech*, *47*, 93–112.

32. Graves, R.C., & Davidoff, L.M. (1924). Studies on the ureter and bladder with especial reference to regurgitation of vesical contents. *Journal of Urology*, *12*, 93.

33. Hutch, J.A. (1967). Vesico-ureteral reflux. In Bergman (Ed.) *The Ureter, Harper and Row* (pp. 465–507).

34. Gruber, C.M. (1929). A comparative study of the intravesical ureters in man and in experimental animals. *Journal of Urology*, *12*, 567.